Journal of Rock Mechanics and Geotechnical Engineering 9 (2017) 490–501

Contents lists available at ScienceDirect

Journal of Rock Mechanics and Geotechnical Engineering

journal homepage: www.rockgeotech.org

Full Length Article

Numerical investigation of the stresses in backfilled stopes overlying a sill mat

Mohamed Amine Sobhi, Li Li*

Research Institute on Mines and the Environment, Department of Civil, Geological and Mining Engineering, École Polytechnique de Montréal, Montréal, Canada

ARTICLE INFO

Article history:
Received 12 July 2016
Received in revised form
28 January 2017
Accepted 30 January 2017
Available online 13 May 2017

Keywords:
Mine depth
Backfill
Sill mat
Stresses
Numerical modeling

ABSTRACT

Backfill is commonly used in underground mines to help increase the ore recovery rate and reduce the ore dilution. The use of a part of mine waste as underground backfill material also helps reduce the environmental impact of mining operations. After all, backfill is used to provide a working platform or safer working space. Its primary and most important role is to improve the rock mass stability around mine openings. However, most available solutions to stress analyses were developed for an isolated stope, without taking into account the influence of mine depth, or of adjacent stopes. In this paper, results from a numerical study carried out to evaluate the stresses in backfilled stopes overlying a sill mat are presented. Mine depth and excavation of the underlying stope below the sill mat (horizontal pillar) are both taken into consideration. The influence of stope geometry, backfill, sill mat and rock properties on the stresses is also evaluated. Compared with the case of a single isolated backfilled stope, the numerical results show that the stress magnitudes in the overlying backfill are considerably increased due to the excavation of the underlying stope. In general, the stresses also increase with mine depth and backfill stiffness, while these tend to decrease with an increase in the surrounding rock mass stiffness. These results suggest that existing solutions for backfill design may need to be revised.

1. Introduction

Backfilling has become very common in underground mines around the world because it helps improve ground stability. It can also reduce the environmental impact of mining operations by utilizing a part of mine waste as underground backfill material (e.g. Aubertin et al., 2002; Bussière, 2007; Benzaazoua et al., 2008).

Several mining methods can involve the use of backfill. For instance, sill mats made of cemented backfill are commonly used to recover sill pillars in sublevel stoping methods. In the case of the underhand cut-and-fill mining method, ore is mined out by horizontal layers (cuts) from a higher level, followed by the construction of sill mats (horizontal pillars) made of cemented backfill. These man-made pillars are designed to provide a safer working space during the mining operations of underlying stopes (Hartman, 1992; Darling, 2011).

A main concern for the design of these sill mats is the minimum required strength of the cemented backfill used for their construction. The only available solutions to determination of the required strength of cemented backfill for sill mats are those of Mitchell (1991) who considered four failure mechanisms by sliding, flexion, rotation, and caving. An equation has been presented for each failure mechanism. The determination of the vertical stress σ_v (kPa) due to the overlying backfill on the cemented backfill sill mat is required in the first three failure modes. Mitchell (1991) proposed the following equation to calculate this stress:

$$\sigma_v = \frac{\gamma B}{2K \tan \phi} \quad (1)$$

where γ and ϕ are the unit weight (kN/m^3) and friction angle of the overlying backfill, respectively; B is the width (m) of the stope (or span of the sill mat); and K is the lateral earth pressure coefficient of the overlying backfill. This equation has been obtained by considering the arching solution for the case of a vertical stope with an

* Corresponding author. Fax: +1 514 340 4477.
E-mail address: li.li@polymtl.ca (L. Li).

Peer review under responsibility of Institute of Rock and Soil Mechanics, Chinese Academy of Sciences.

http://dx.doi.org/10.1016/j.jrmge.2017.01.001

infinite backfill thickness. Following the approach of Terzaghi (1943) for the case of an excavation within a cohesive soil (known as the "trap-door" problem), Mitchell (1991) has assumed $K = 1$.

1.1. Stresses in backfilled stopes

The stress distribution in a backfilled stope has been investigated extensively over the last decade or so. A few analytical solutions have been proposed for evaluating the stresses within two-dimensional (2D) and three-dimensional (3D) vertical (Aubertin et al., 2003; Li et al., 2005; Pirapakaran and Sivakugan, 2007a; Sobhi et al., 2017) and inclined (Caceres, 2005; Ting et al., 2011, 2014; Jahanbakhshzadeh et al., 2017) backfilled stopes. The non-uniform distribution of the stresses along the width of backfilled stopes has also been taken into account (Li and Aubertin, 2008, 2010), as well as the pore water pressure (Li and Aubertin, 2009a,b, 2010). All of these solutions are extensions from the approach of Marston (1930) who made use of Janssen's (1895) arching theory for estimating the loads on buried conduits in trenches. Arching in backfilled openings has been confirmed by numerical modeling (Li et al., 2003; Pirapakaran and Sivakugan, 2007a; Li and Aubertin, 2009c; Veenstra et al., 2014a, b; Widisinghe et al., 2014) and experimental results (Take and Valsangkar, 2001; Belem et al., 2004; Grabinsky, 2010; Pirapakaran and Sivakugan, 2007b; Thompson et al., 2012; Ting et al., 2012; Widisinghe et al., 2013, 2014; Li et al., 2014).

1.2. Limitations of existing solutions

It is noted that all of the previous numerical, analytical and laboratory experimental investigations were performed without considering the excavation (and filling) of neighboring stopes, except for Hill et al. (1974), Pariseau et al. (1976), Beruar et al. (2013) and Falaknaz et al. (2015a, b). Hill et al. (1974) and later Pariseau et al. (1976) conducted a few finite element analyses to investigate the effect of backfilling on the stope closure and stresses in a sill pillar separating two stopes. They indicated that the stope closure and pillar stresses can be decreased significantly by using a stronger backfill. Beruar et al. (2013) investigated the influence of sill pillar geometry and addition of backfill on the rockburst potential of pillars. Their results did not include the stresses in the backfill. Falaknaz et al. (2015a,b) investigated the stresses in multiple backfilled stopes laying side by side (at the same level). Their results showed that the stress distributions within a backfilled stope can be quite different when a new stope is created nearby.

In this paper, the stress distribution along the vertical central line (VCL) of a backfilled stope overlying a sill mat made of cemented backfill is investigated before and after the excavation of a stope underneath. The focus is placed on the influences of the stope depth and geometry and of the mechanical properties of the backfill, sill mat and rock mass on the induced stresses.

2. Numerical modeling

2.1. Numerical model

The numerical study was carried out using the finite element software PLAXIS 2D (Brinkgreve et al., 2014). The validation process before its application to the present investigation can be found in Sobhi (2014).

Fig. 1 shows the model of a sill mat with an overlying uncemented backfill and an excavation underneath. B is the stope (and sill mat) width, H is the height of the overlying backfill, and e is the thickness of the sill mat. The backfill, sill mat and rock mass are considered as homogeneous and isotropic materials obeying the elasto-plastic law with Coulomb criterion.

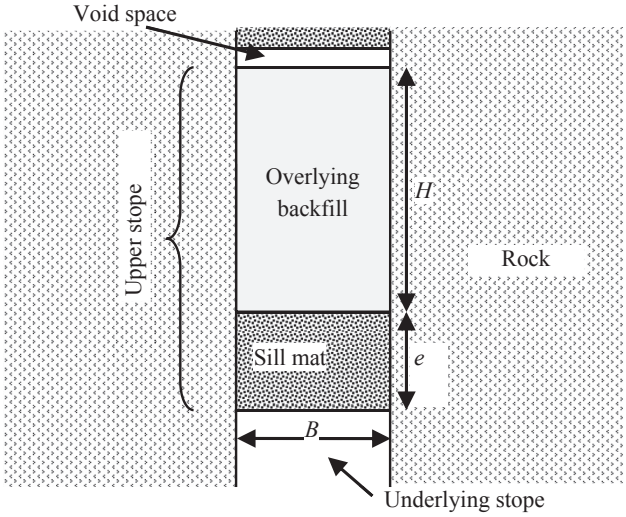

Fig. 1. Model of a sill mat with an overlying uncemented backfill of height H and an underlying excavation.

Parameter sensibility analyses were performed with a reference configuration. It consists of a 6 m wide and 3 m thick sill mat and an overlying vertical stope filled with a cohesionless backfill characterized by $H = 10$ m (height), $E = 300$ MPa (Young's modulus), $\mu = 0.3$ (Poisson's ratio), $\gamma = 18$ kN/m^3 (unit weight), $\phi = 35°$ (friction angle), and $\psi = 0°$ (dilation angle). For the sill mat, the Young's modulus $E_s = 5$ GPa, Poisson's ratio $\mu_s = 0.3$, unit weight $\gamma_s = 20$ kN/m^3, cohesion $c_s = 1500$ kPa, friction angle $\phi_s = 35°$, and dilation angle $\psi_s = 0°$. As for the surrounding rock mass, the Young's modulus $E_r = 42$ GPa, Poisson's ratio $\mu_r = 0.25$, unit weight $\gamma_r = 27$ kN/m^3, cohesion $c_r = 9400$ kPa, friction angle $\phi_r = 38°$, and dilation angle $\psi_r = 0°$. A void space of 0.5 m is left between the top surface of the backfill and the back of the stope to simulate the poor contact between the backfill and stope roof. The sill mat is located at a depth $z = 200$ m from its mid-height to the ground surface. A typical stress regime of the Canadian Shield is applied to the rock mass (Herget, 1988; Arjang, 2004), where the vertical in-situ stress is calculated based on the overburden and the horizontal natural stress is twice the vertical in-situ stress (i.e. with a lateral earth pressure coefficient of the rock mass $K_r = 2$).

Fig. 2 shows the typical numerical model built with PLAXIS 2D for a vertical backfilled stope overlying the sill mat. The vertical symmetry axis has been taken into account by using only half of the full model. The outer boundary is free along the upper face to simulate the ground surface, fixed in the horizontal direction but free in vertical direction along the lateral face, and fixed in both the vertical and horizontal directions along the lower face. The input data for the reference case are also presented in Fig. 2. Other simulations have been conducted by changing one parameter at each time to see its influence on the stress distribution within the backfilled stope and the sill mat.

The numerical simulations have been conducted by following the five steps shown in Fig. 3. The first step is to obtain an initial stress state in the model before any opening exists. The second step consists of excavating the upper stope. In step 3, a sill mat is added using a cemented backfill. A cohesionless backfill material is added (in one layer) above the sill mat in step 4. The last step (step 5) is the creation of a stope below the sill mat.

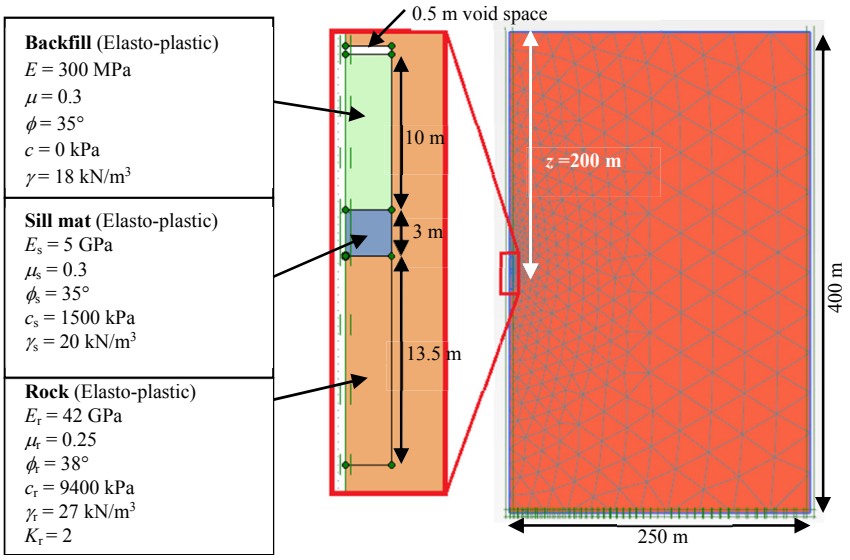

Fig. 2. Reference model of the sill mat with an overlying backfill and an underlying excavation, built with PLAXIS 2D.

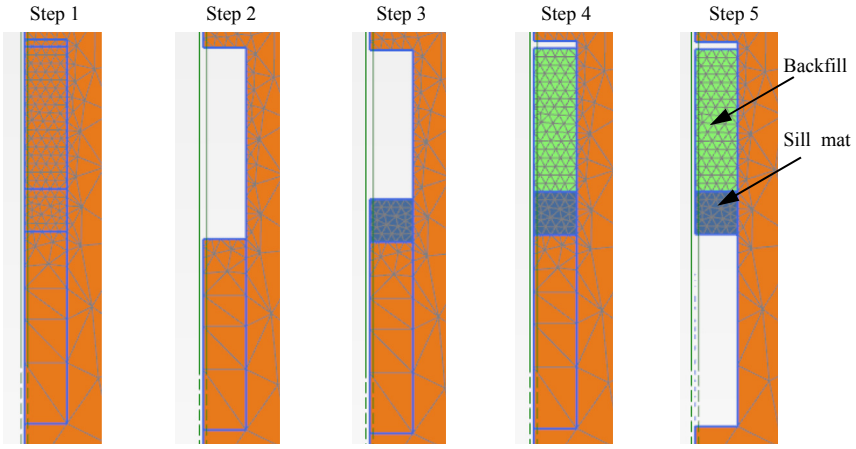

Fig. 3. Steps followed for the numerical simulations.

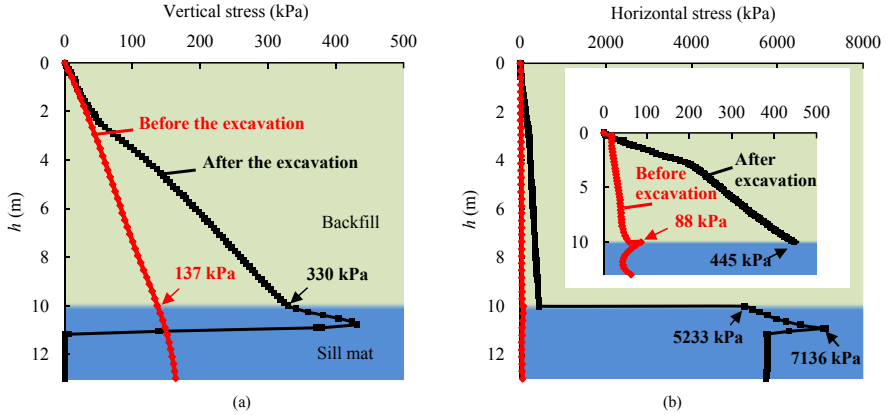

Fig. 4. Variations of the (a) vertical and (b) horizontal stresses along the VCL of the backfilled stope for the reference case before and after the excavation of the underlying stope (see the properties given in Fig. 2).

2.2. Numerical results

Fig. 4 shows the vertical (Fig. 4a) and horizontal (Fig. 4b) stresses for the reference case (obtained from PLAXIS 2D) along the VCL of the upper stope, before and after the excavation of the underlying stope. Before the excavation of this stope, the vertical stress tends to increase smoothly and nonlinearly with depth within the overlying backfill and sill mat, reaching 137 kPa at the top and 164 kPa at the bottom of the sill mat. The effect of arching is observed from the nonlinear variation between the stresses and depth within both the overlying backfill and sill mat. After the excavation of the underlying stope, the vertical stress σ_v (Fig. 4a) increases linearly with the depth h; this increase is about 20 kPa/m (close to overburden) in the upper part of the stope ($h < 2.5$ m), and then becomes ~36 kPa/m up to about 330 kPa at the interface with the sill mat. In the sill mat, it keeps increasing in an even larger rate to a peak value of 430 kPa before declining quickly to zero (further addressed in "Discussion") at one third of the sill mat thickness.

Fig. 4b indicates that the horizontal stress σ_h before the excavation of the underlying stope tends to increase nonlinearly with depth, reaching a maximum value of about 60 kPa at the base of the backfill. Within the sill mat, it jumps to 88 kPa at the top and diminishes to a minimum of 45 kPa, 1 m above the base. After the excavation of the underlying stope, the horizontal stress increases gradually with depth to about 445 kPa at the base of the backfill. Within the sill mat, it jumps to a value of about 5200 kPa at the top of the sill mat and increases to a peak value of about 7000 kPa before declining slightly around mid-height and stabilizing at a value of about 5800 kPa.

These results indicate that the excavation of the underlying stope results in an increase of the vertical stress in the overlying backfill and in an increase of the horizontal stress in the sill mat.

It is also noticed that the vertical stress σ_v within the overlying backfill and sill mat is significantly lower than the horizontal stress σ_h. This tendency is considerably different from that of an isolated stope with delayed backfilling (Li et al., 2003, 2005; Li and Aubertin, 2009c; Sobhi, 2014). These results indicate that the stope excavation below the sill mat changes significantly the stress state within the overlying backfill and the sill mat. These stress changes were not considered in existing solutions for sill mat design (Mitchell, 1991).

Fig. 5 is an enlarged view of Fig. 4, showing the vertical (Fig. 5a) and horizontal (Fig. 5b) stress distributions along the VCL of the overlying backfill before and after the excavation of the underlying stope. The results obtained by applying the Marston solution (Aubertin et al., 2003) are also plotted in the figure. It is seen that the numerical results obtained prior to the excavation of the underlying stope correspond quite well to those predicted by the analytical solution presented by Aubertin et al. (2003). The creation of a stope below the sill mat results in a significant increase of the stresses along the VCL of the overlying stope. For the reference case, the horizontal stress σ_h becomes 7.5 times larger (from 59 kPa to 445 kPa), whereas the vertical stress σ_v increases by almost 2.5 times (from 137 kPa to 330 kPa) in the lower portion of the backfill. This significant increase in stresses is probably induced by the closure of the stope walls due to the excavation of the underlying stope. This stope closure can be observed from Fig. 6, which presents the iso-contours of the horizontal displacement obtained by PLAXIS before and after the excavation of the underlying stope. The horizontal displacements after the excavation of the underlying stope are much larger than those before excavation.

In the following subsections, the influences of the stope depth and geometry, and of the backfill, sill mat and rock mass properties on the stresses are investigated numerically.

2.2.1. Influence of the stope depth

Fig. 7 shows the variations of the horizontal (Fig. 7a) and vertical (Fig. 7b) stresses along the VCL of the upper stope when the mine depth z varies from 0 to 400 m beneath the ground surface. The vertical and horizontal stresses increase proportionally with the increase of mine depth up to 150 m. At the bottom of the backfill, for instance, when the depth increases from 0 to 150 m, the horizontal stress increases by 3 times (from 118 kPa to 348 kPa) and the vertical stress increases by almost 2 times (from 149 kPa to 253 kPa). Beyond that depth, the stresses within the overlying backfill and in the upper part of the sill mat increase also considerably when the depth increases from 200 m to 300 m, but tend to stabilize with a further increase in the mine depth from 300 m to 400 m. In the lower part of the sill mat, a sudden drop is observed in the horizontal and vertical stresses when the mine stope is located at a depth greater than 200 m. This probably results from the yield of the cemented backfill, as shown in Fig. 8 (further addressed in "Discussion").

2.2.2. Influence of the stope geometry

Fig. 9 shows the variations of the horizontal (Fig. 9a) and vertical (Fig. 9b) stresses along the VCL of the upper stope with the stope width B varying between 4 m and 10 m. In general, the stresses within the overlying backfill and sill mat decrease with a wider stope. But the vertical stress σ_v tends to become insensitive to the further variation of B once $B \geq 8$ m.

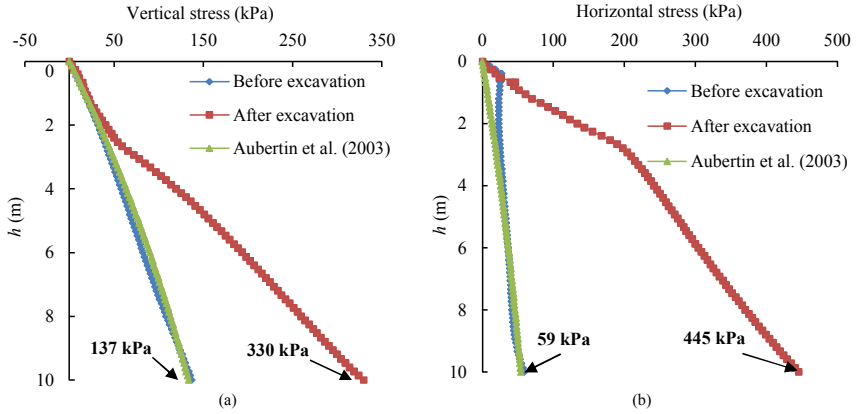

Fig. 5. Variations of the (a) vertical and (b) horizontal stresses along the VCL of the overlying backfill for the reference model before and after the excavation of the underlying stope.

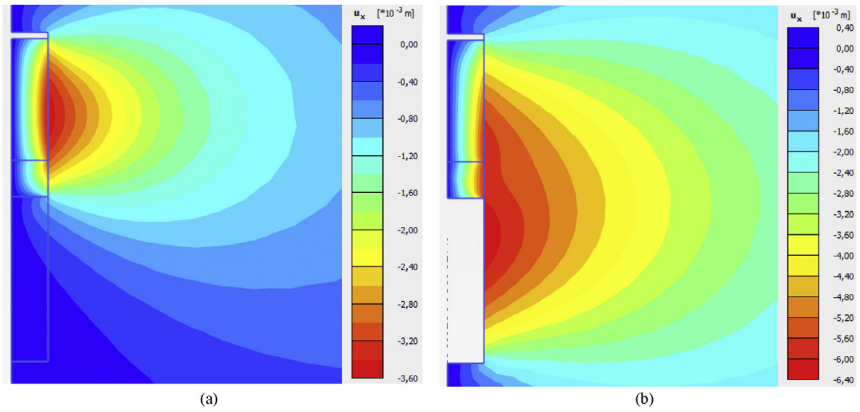

Fig. 6. Iso-contours of the horizontal displacements obtained with PLAXIS for the case of reference (a) before and (b) after the excavation of the underlying stope.

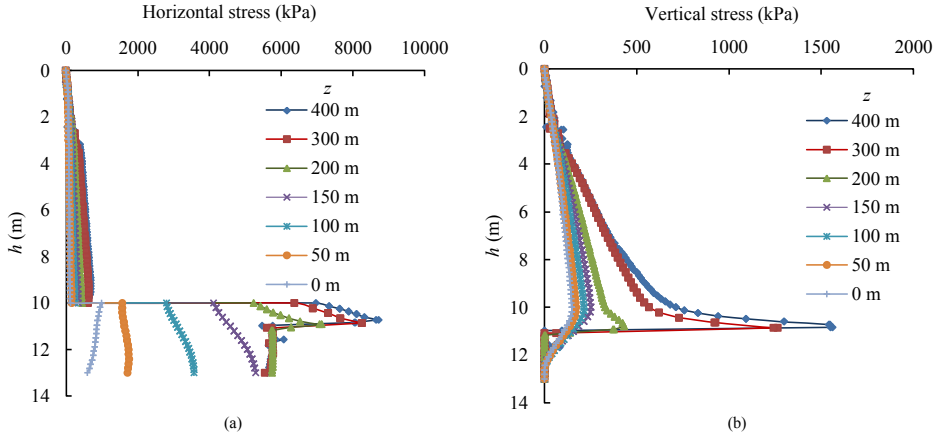

Fig. 7. Variations of (a) horizontal and (b) vertical stresses along the VCL of the backfilled stope located at different depths z; other parameters are given in Fig. 2.

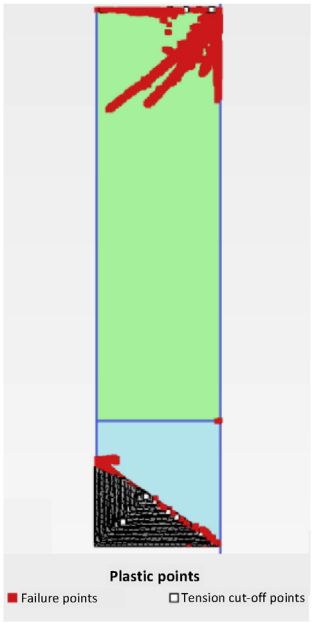

Fig. 8. Yield state of the overlying backfill and sill mat for the reference case.

These results are very different from those with an isolated stope. In the latter case, the stresses generally increase with an increase in stope width due to reduction of arching effect. Here, the stresses are mostly due to the compression by stope closure. With a wider stope, the average strain (roughly estimated as the ratio of the stope closure to the stope width) becomes smaller, leading to reduced stresses in the overlying backfill.

Fig. 10 presents the stress variations along the central line of the upper stope when the inclination angle of the stope walls α varies from 90° to 50°. In the overlying backfill, the horizontal stress σ_h (Fig. 10a) is not very sensitive to the variation of the stope inclination angle α. But the vertical stress σ_v (Fig. 10b) increases when the stope walls are more inclined from the vertical. For example, the peak value of the vertical stress in the sill mat increases by almost 4 times (from 431 kPa to 1851 kPa) when the stope inclination is reduced from 90° (vertical) to 50°. This is probably due to the fact that the vertical component of the wall closure increases with a reduced inclination angle α, resulting in larger vertical stress in the backfilled stope.

2.2.3. *Influence of the mechanical properties of the overlying backfill*

Fig. 11 shows the variations of the horizontal (Fig. 11a) and vertical (Fig. 11b) stresses along the VCL of the upper stope with different Young's moduli E of the backfill. It is seen that the stresses within the overlying backfill increase considerably with an

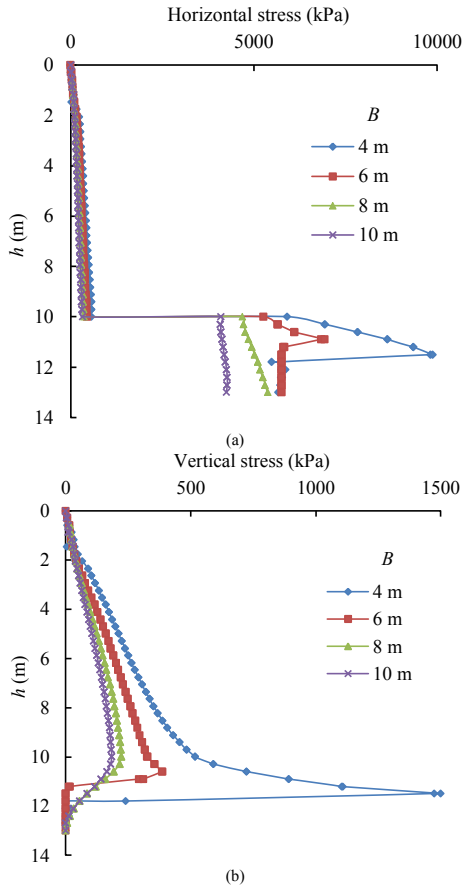

Fig. 9. Variations of the (a) horizontal and (b) vertical stresses along the VCL of the backfilled stope with different stope widths B; other parameters are given in Fig. 2.

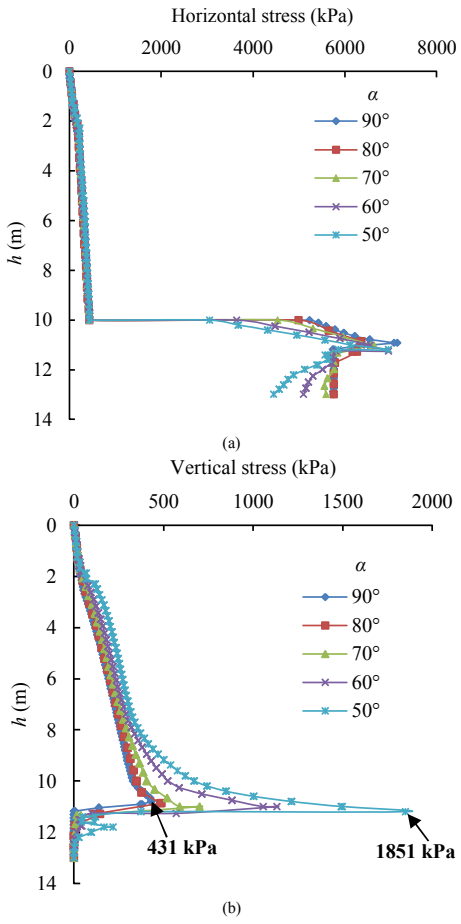

Fig. 10. Variations of the (a) horizontal and (b) vertical stresses along the central line of the backfilled stope with different stope wall inclination angles α; other parameters are given in Fig. 2.

increased value of this parameter. At the bottom of the backfill, for example, the horizontal stress σ_h increases by almost 8 times (from 99 kPa to 819 kPa) when the Young's modulus E is increased from 30 MPa to 600 MPa. In the sill mat, the horizontal stress σ_h (Fig. 11a) is not very sensitive to the variation of E, while the peak value of the vertical stress σ_v (Fig. 11b) increases by 2 times (from 236 kPa to 478 kPa) when the Young's modulus E increases from 30 MPa to 600 MPa. These results are closely related to the yield of the sill mat and further addressed in the Subsection 2.2.5.

A similar tendency has been observed for the variation of the horizontal and vertical stresses along the VCL of the upper stope when the Poisson's ratio of the backfill μ varies between 0.2 and 0.4, as shown in Fig. 12. The horizontal stress σ_h (Fig. 12a) and vertical stress σ_v (Fig. 12b) increase in the overlying backfill with an increase in Poisson's ratio μ. In the sill mat, the horizontal stress is insensitive to the variation of μ, while the vertical stress increases with an increase in Poisson's ratio μ.

The influence of the backfill's friction angle ϕ on the stresses in the overlying backfill and sill mat has also been investigated. The results (not shown here; see Sobhi, 2014) suggest that this parameter has no effect on the stress distributions along the VCL of the upper stope.

2.2.4. Influence of the mechanical properties of the sill mat

Fig. 13 shows the variations of the stresses along the VCL of the upper stope with different Young's moduli of the sill mat E_s. An increase in E_s results in a considerable increase of the horizontal and vertical stresses along the VCL of the sill mat. For example, in the upper part of the sill mat, the horizontal stress σ_h increases by almost 7 times (from 832 kPa to 5930 kPa) and the vertical stress σ_v by almost 4 times when the Young's modulus of the sill mat E_s increases from 500 MPa to 10 GPa. But the stresses tend to stabilize in the lower part of the sill mat when the value of E_s exceeds 5 GPa, probably due to the yield of the cemented material as shown in Fig. 8. In the overlying backfill, an increase of E_s leads to a slight decrease in the horizontal stress σ_h (Fig. 13a) and an increase in the vertical stress σ_v (Fig. 13b). A stiffer sill mat supports larger stresses and reduces the stope closure on the overlying backfill, resulting in a decreased horizontal stress in the overlying backfill. Regarding the increase of the vertical stress in the overlying backfill (also in the upper part of the sill mat) with an increased sill mat stiffness, it can be due to the increase in the vertical deformation associated with increase in the horizontal stress in the upper part of the sill mat through the Poisson's effect. This is partly confirmed by the results shown in Fig. 14.

Fig. 14 shows the variations of the stresses along the VCL of the upper stope as a function of the sill mat Poisson's ratio μ_s ranging from 0.2 to 0.4. One can see that the variation of the Poisson's ratio μ_s has a minor effect on the horizontal stress σ_h (Fig. 14a) within the overlying backfill. But its increase can lead to an increase in the vertical stress within the overlying backfill (Fig. 14b) and an increase in the horizontal and vertical stresses in the upper part of the sill mat. These increases can be explained by the fact that the vertical deformation (swelling) of the sill mat tends to increase with an increased μ_s. This increase combined with the confining effect of

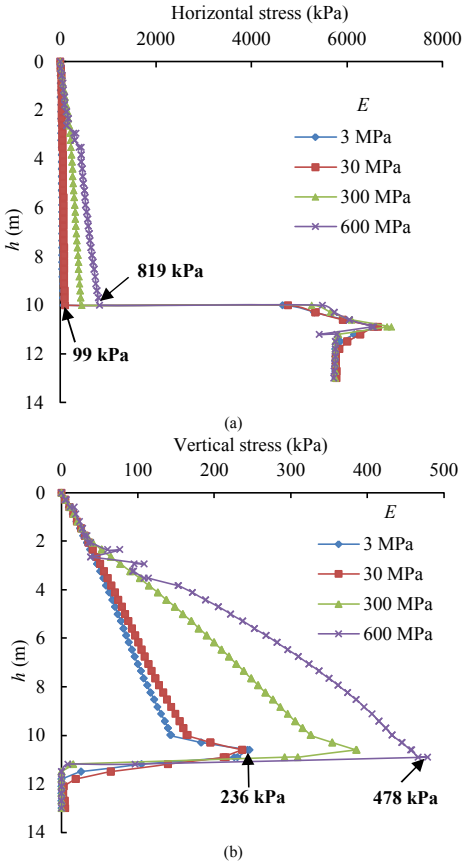

Fig. 11. Variations of the (a) horizontal and (b) vertical stresses along the VCL of the backfilled stope with different backfill's Young's moduli E; other parameters are given in Fig. 2.

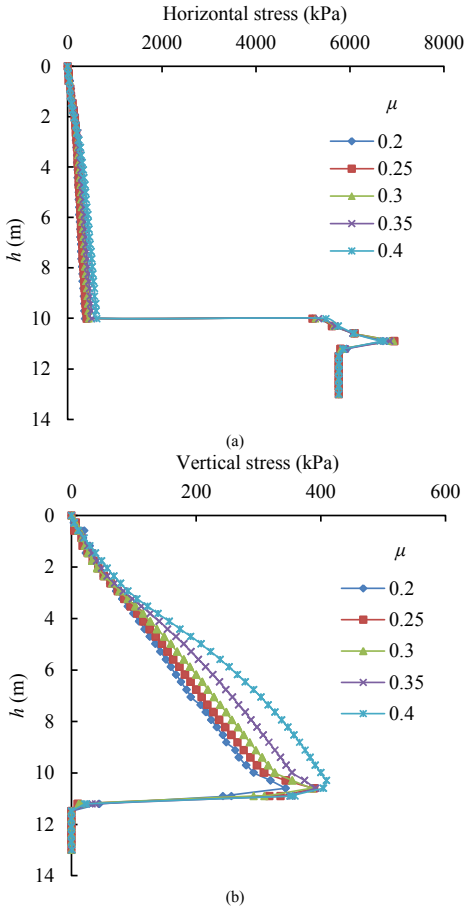

Fig. 12. Variations of the (a) horizontal and (b) vertical stresses along the VCL of the backfilled stope with different backfill's Poisson's ratios μ; other parameters are given in Fig. 2.

the overlying backfill results in an increase in the vertical stress at the lower part of the overlying backfill and upper part of the sill mat, which in turn has an effect to increase the strength of the sill mat. The horizontal stress σ_h in the sill mat can thus be increased in the upper part of the sill mat.

Figs. 15 and 16 show the variations of the stresses in the upper stope with different internal friction angles ϕ_s and cohesions c_s, respectively. It can be seen that the variation of the shear strength parameters has little effect on the horizontal stress within the overlying backfill. But a stronger sill mat can bear higher (deviatoric) stresses. Accordingly, the horizontal stress σ_h in the lower part of the sill mat increases with an increase in the friction angle (Fig. 15a) and cohesion (Fig. 16a) of the sill mat. This results in a reduction of plastic (swelling) deformations, which in turn leads to a decrease of the vertical stress σ_v in the overlying backfill and the upper part of the sill mat (Figs. 15b and 16b).

2.2.5. *Influence of the mechanical properties of the rock mass*

The variations of the stresses along the VCL of the upper stope with the Young's modulus E_r of the rock mass are presented in Fig. 17. It is seen that the horizontal (Fig. 17a) and vertical (Fig. 17b) stresses decrease with an increase in E_r. At the bottom of the backfill, for example, the vertical stress σ_v decreases by almost 2.5 times (from 682 kPa to 266 kPa) when E_r changes from 20 GPa to 50 GPa. This is quite straightforward. With a stiffer rock mass, the wall deformation and closure would be smaller, resulting in smaller horizontal and vertical stresses within the overlying backfill and sill mat. A similar trend has been observed for the variation of the stresses within the backfilled stope when the Poisson's ratio μ_r of the rock mass increases from 0.2 to 0.4, as shown in Fig. 18.

The influence of the shear strength parameters ϕ_r and c_r of the rock mass on the stresses within backfilled stope has also been investigated. The results (not shown here; see Sobhi, 2014) indicate that these two parameters have little effect on the stresses when ϕ_r varies from 25° to 40° and c_r from 2000 kPa to 11,000 kPa. These results are not expected because an increase in the shear strength of the rock mass would have the effect to reduce the plastic zones around the stope and result in smaller stresses in the overlying backfill and sill mat. This is probably due to the stress state mostly in tension around the stope and the application of Mohr-Coulomb model with a zero tensile strength cut-off. The yield zones by tension, as shown in Fig. 8, are independent of the two shear strength parameters.

Fig. 19 shows the variations of the stresses in the backfilled stope as the lateral earth pressure coefficient of the rock mass K_r changes from 0.5 to 4. As expected, an increase in K_r leads to a significant increase in the horizontal (Fig. 19a) and vertical (Fig. 19b) stresses within the overlying backfill and sill mat. An increased K_r means an increased initial horizontal rock stress and larger rock wall closure accompanied with the underlying excavation. It is straightforward to understand the increase in the horizontal stress in the sill mat and overlying backfill as K_r increases. Near the upper part of the sill mat, the vertical stress of the overlying backfill plays the role of confining pressure. It has effect to increase the shear strength of the sill mat material. The horizontal stress can thus increase as K_r increases from 0.5 to 4. Near the lower part of the sill mat, the confining pressure provided by the vertical stress remains to be zero on the base surface

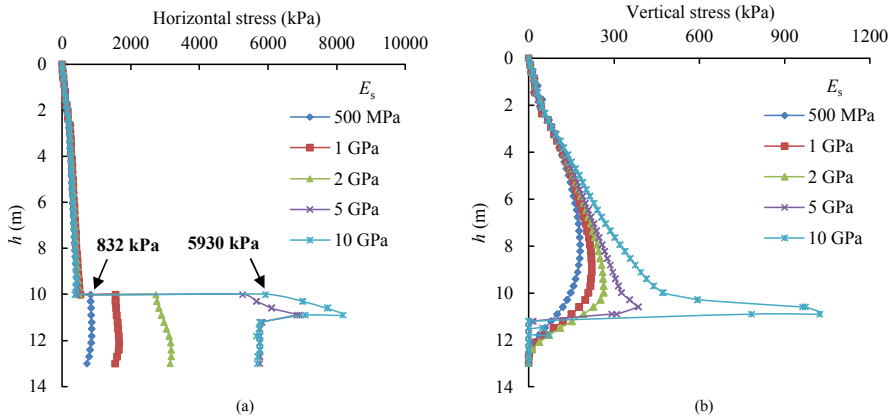

Fig. 13. Variations of the (a) horizontal and (b) vertical stresses along the VCL of the backfilled stope with different Young's moduli of the sill mat E_s; other parameters are given in Fig. 2.

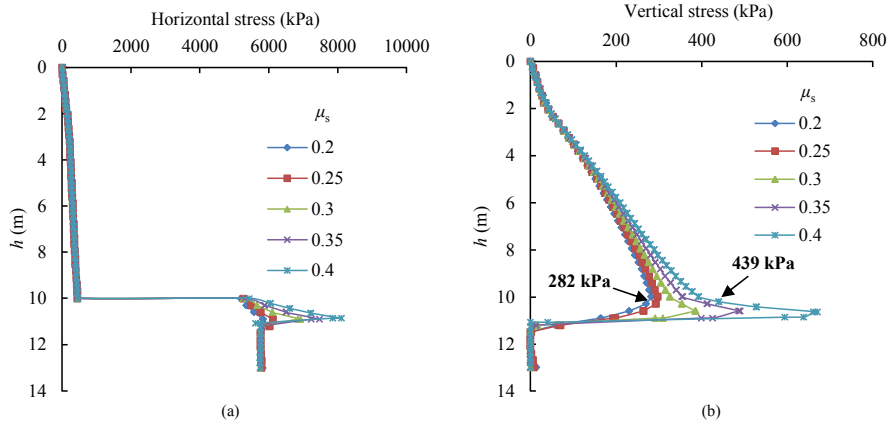

Fig. 14. Variations of the (a) horizontal and (b) vertical stresses along the VCL of the backfilled stope with different Poisson's ratio of sill mat μ_s; other parameters are given in Fig. 2.

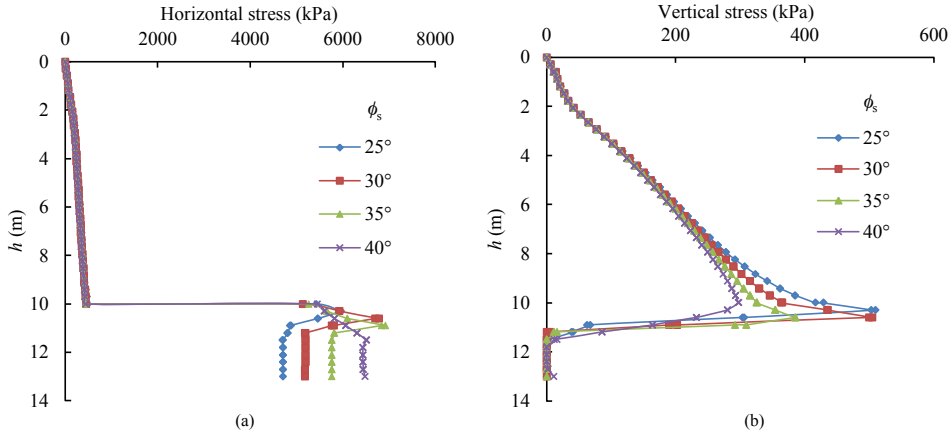

Fig. 15. Variations of the (a) horizontal and (b) vertical stresses along the VCL of the backfilled stope with different friction angles of sill mat ϕ_s; other parameters are given in Fig. 2.

and very small inside the base part of the sill mat. The horizontal stress increases as long as the material of the sill mat is unyielding when K_r increases from 0.5 to 2. With further increase of K_r from 2 to 4, the material of the sill mat yields and the horizontal stress does not change anymore (due to the elasto-plastic Mohr-Coulomb model). These results indicate that the lower part of the sill mat is more vulnerable (unstable) than elsewhere (upper part of the sill mat).

Regarding the increase of the vertical stress in the sill mat and overlying backfill, this should be due to the Poisson's effect in the vertical direction by the increased horizontal stress with the increased K_r.

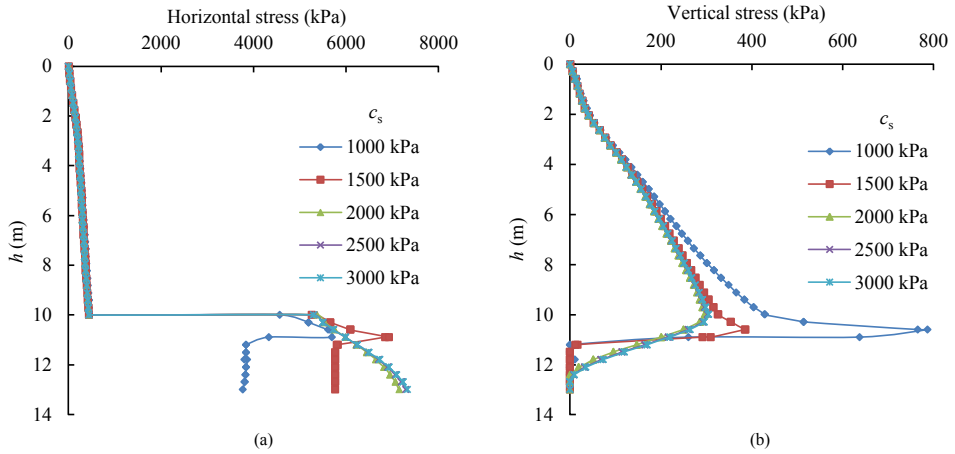

Fig. 16. Variations of the (a) horizontal and (b) vertical stresses along the VCL of the backfilled stope with different cohesions of sill mat c_s; other parameters are given in Fig. 2.

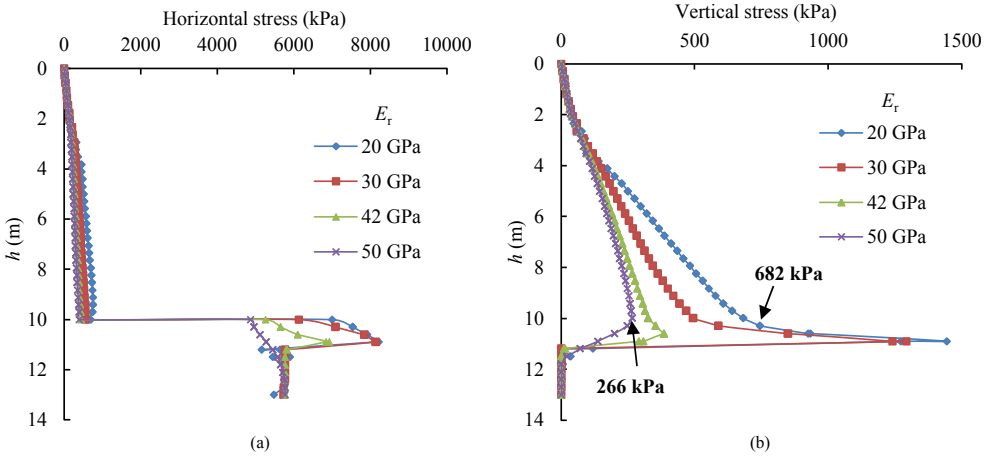

Fig. 17. Variations of the (a) horizontal and (b) vertical stresses along the VCL of the backfilled stope with different Young's moduli of the rock mass E_r; other parameters are given in Fig. 2.

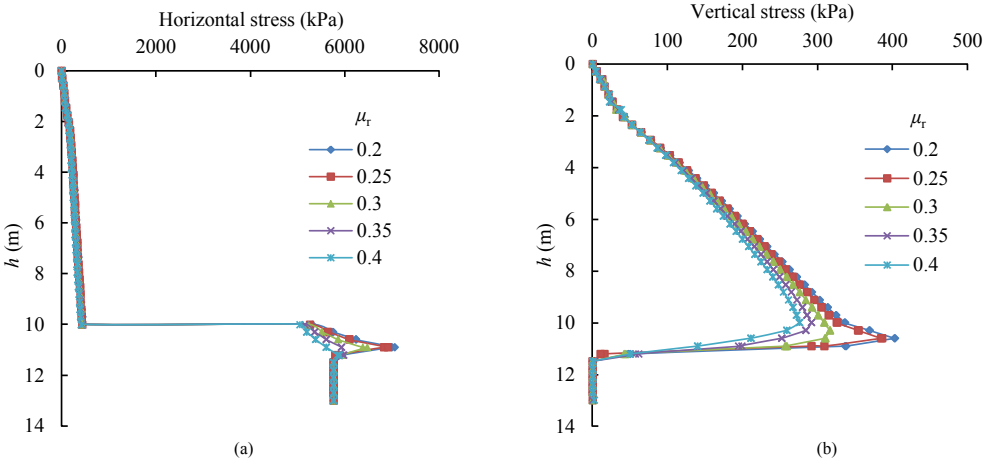

Fig. 18. Variations of the (a) horizontal and (b) vertical stresses along the VCL of the backfilled stope with different Poisson's ratios of the rock mass μ_r; other parameters are given in Fig. 2.

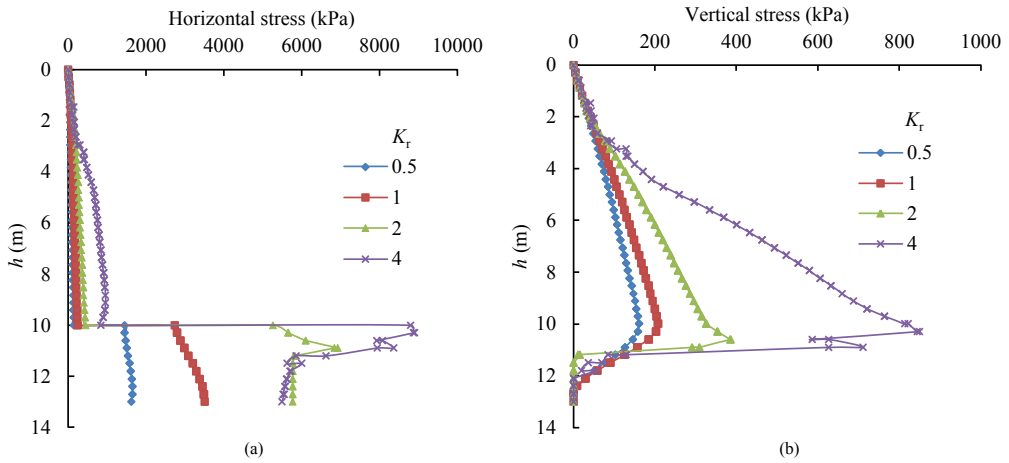

Fig. 19. Variations of the (a) horizontal and (b) vertical stresses along the VCL of the backfilled stope with different lateral earth pressure coefficients of the rock mass K_r; other parameters are given in Fig. 2.

3. Discussion

A series of numerical simulations has been performed to investigate the stress distribution within a backfilled stope (including the overlying backfill and sill mat) after the creation of a stope underneath. It should be reminded that the numerical models presented in this paper are 2D (plane strain). The results and conclusions are mostly valid for the case of very long stopes in the third dimension.

Another limitation is related to the one layer placement of the overlying backfill above the sill mat. This manner of backfilling can slightly overestimate the stresses due to the dynamic response of the backfill (Pirapakaran and Sivakugan, 2007a; Li and Aubertin, 2009c), as shown in Fig. 5b, where the horizontal stress obtained by the numerical modeling is higher than that predicted by the analytical solution of Aubertin et al. (2003).

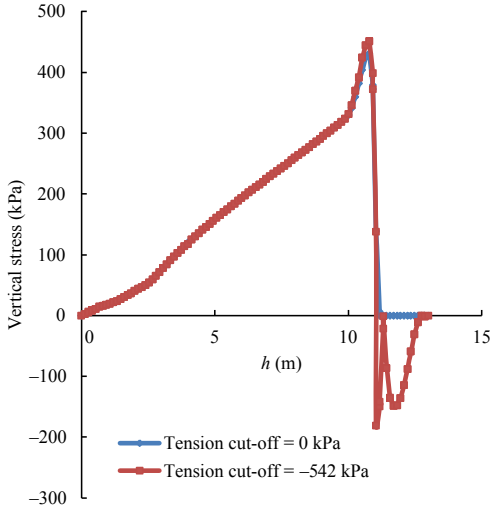

Fig. 20. Variations of the vertical stress along the VCL of the upper stope, obtained by applying the Mohr-Coulomb model with zero and nonzero tensile strength cut-off for the reference case (see Fig. 2).

One notes that the sill mat and the surrounding rock mass reach a yield state when the stope is located at a depth only greater than 200 m (Fig. 8). This is mostly due to the stress state in tension around the stope and the application of the Mohr-Coulomb model with a zero tensile strength cut-off. Probably because of this, no tensile stresses appear around the stope and in the sill mat. When the Mohr-Coulomb model with a nonzero tensile strength cut-off is applied to the sill mat, tensile stresses appear at the lower part of the sill mat, as shown in Fig. 20. Nevertheless, it is expected that the trends of the stress variation with the diverse parameters represent well the behaviors of the overlying backfill and sill mat upon the excavation of the stope underneath. These results suggest that the lower part of the sill mat is more vulnerable (unstable) than the upper part. In sill mat design, the reinforcement of the lower part should be considered.

In the numerical model, a void of 0.5 m was considered at the top of overlying backfill to simulate a poor contact between the backfill and the back of the stope. This may have effect to underestimate the vertical and horizontal stresses in the overlying backfill and sill mat. More work is needed in this aspect.

It is well-known that the Mohr-Coulomb criterion is not always appropriate for cohesive geomaterials when dealing with tension or high compression stress state. In this regard, Li and his coworkers have developed an elasto-plastic model using a multiaxial criterion that can be used to estimate the stresses in backfilled stopes (Li and Aubertin, 2009d; Li et al., 2010).

Other factors that can be considered in the future include the pore water pressure (Li and Aubertin, 2009a, b, 2010), backfill drainage and consolidation (El Mkadmi et al., 2014; Shahsavari and Grabinsky, 2014), strength evolution of the backfill with curing time (Godbout et al., 2007), dynamic loading (Shahsavari et al., 2014), etc.

4. Conclusions

The stresses within the overlying backfill and sill mat are analyzed by numerical modeling performed with PLAXIS by considering the excavation of a stope underneath. In the overlying backfill, the stresses are significantly increased due to the excavation of the underlying stope. Within the sill mat, the horizontal stress generally shows an increase while the vertical stress gener-

ally shows a decrease (especially at the lower part) after the creation of the stope underneath. These changes need to be carefully taken into account in backfill and barricade design.

The results also suggest that the lower part of the sill mat is more vulnerable. In sill mat design, the reinforcement of the lower part by using higher cement content or by adding wire mesh should be considered to improve the stability of the sill mat.

The results further show that the vertical and horizontal stresses within the overlying backfill increase with the stope depth, earth pressure coefficient of the natural rocks, and the overlying backfill's stiffness and Poisson's ratio. For the given properties and geometry, the results show that the stresses within the overlying backfill are not very sensitive to the change in the friction angle of the overlying backfill and shear strength (cohesion and friction angle) of the rock mass. The vertical and horizontal stresses within the overlying backfill decrease with an increase in the stope width, stope wall inclination angle, rock mass stiffness, or sill mat shear strength (cohesion and friction angle). Within the overlying backfill, the vertical stress increases with an increase in the stiffness and Poisson's ratio of the sill mat, whereas the horizontal stress is not sensitive to the change in the Poisson's ratio of the sill mat and decreases with an increase in the stiffness of the sill mat.

Conflict of interest

The authors wish to confirm that there are no known conflicts of interest associated with this publication and there has been no significant financial support for this work that could have influenced its outcome.

Acknowledgment

The authors acknowledge the financial support of the Natural Sciences and Engineering Research Council of Canada (NSERC 402318), Institut de recherche Robert-Sauvé en santé et en sécurité du travail (IRSST 2013-0029), Fonds de recherche du Québec – Nature et technologies (FRQNT 2015-MI-191676), and the industrial partners of Research Institute on Mines and Environment (RIME UQAT-Polytechnique, http://rime-irme.ca). Dr. Michel Aubertin is gratefully acknowledged for the reading and discussion on part of the manuscript.

References

Arjang B. Database on Canadian in situ ground stresses. CANMET division report MMSL 01–029. Ottawa, Canada: CANMET; 2004.
Aubertin M, Bernier L, Bussière B. Environnement et gestion des rejets miniers. Mont-Royal, Canada: Presses Internationales Polytechnique; 2002 [CD-ROM].
Aubertin M, Li L, Arnoldi S, Belem T, Bussière B, Benzaazoua M, Simon R. Interaction between backfill and rock mass in narrow stopes. In: Soil and rock America 2003, vol. 1. Essen: Verlag Gluckauf GMBH; 2003. p. 1157–64.
Belem T, Harvey A, Simon R, Aubertin M. Measurement and prediction of internal stresses in an underground opening during its filling with cemented fill. In: Villaescusa E, Potvin Y, editors. Proceedings of the 5th international symposium on ground support mining and underground construction. Rotterdam: A.A. Balkema; 2004. p. 619–29.
Benzaazoua M, Bussière B, Demers I, Aubertin M, Fried É, Blier A. Integrated mine tailings management by combining environmental desulphurization and cemented paste backfill: application to mine Doyon, Quebec, Canada. Minerals Engineering 2008;21(4):330–40.
Beruar O, Thibodeau D, Sharan S, Cai M. Consideration of post-peak response of the pillar-rock system in sill pillar design. In: Proceedings of the 23rd World mining Congress. Canadian Institute of Mining, Metallurgy and Petroleum; 2013.
Brinkgreve RBJ, Engin E, Swolfs WM. PLAXIS 2014. Delft, Netherlands: PLAXIS bv; 2014.
Bussière B. Colloquium 2004: hydro-geotechnical properties of hard rock tailings from metal mines and emerging geo-environmental disposal approaches. Canadian Geotechnical Journal 2007;44(9):1019–52.
Caceres C. Effect of delayed backfill on open stope mining methods. MS Thesis. Vancouver, Canada: University of British Columbia; 2005.
Darling P. SME mining engineering handbook. 3rd ed. Society for Mining, Metallurgy, and Exploration, Inc. (SME); 2011.
El Mkadmi N, Aubertin M, Li L. Effect of drainage and sequential filling on the behavior of backfill in mine stopes. Canadian Geotechnical Journal 2014;51(1):1–15.
Falaknaz N, Aubertin M, Li L. A numerical investigation of the geomechanical response of adjacent backfilled stopes. Canadian Geotechnical Journal 2015a;52(10):1507–25.
Falaknaz N, Aubertin M, Li L. Numerical analyses of the stress state in two neighboring backfilled stopes. International Journal of Geomechanics 2015b;15(6). http://dx.doi.org/10.1061/(ASCE)GM.1943-5622.0000466#sthash.5XXIeIAR.dpuf.
Godbout J, Bussière B, Aubertin M, Belem T. Evolution of cemented paste backfill saturated hydraulic conductivity at early curing time. In: Proceedings of the 60th Canadian geotechnical conference & 8th joint CGS/IAH-CNC groundwater conference. Ottawa, Canada: Canadian Geotechnical Society; 2007. p. 2230–6.
Grabinsky MW. In situ monitoring for ground truthing paste backfill designs. In: Proceedings of the 13th international seminar on paste and thickened tailings. Crawley, Australia: Australian Centre for Geomechanics; 2010. p. 85–98.
Hartman HL. SME mining engineering handbook, vol. 1. SME; 1992.
Herget G. Stresses in rock. Rotterdam: A.A. Balkema; 1988.
Hill JR, McDonald MM, McNay LM. Support performance of hydraulic backfill: a preliminary analysis. US Bureau of Mines; 1974.
Jahanbakhshzadeh A, Aubertin M, Li L. A new analytical solution for the stress state in inclined backfilled mine stopes. Geotechnical and Geological Engineering 2017. http://dx.doi.org/10.1007/s10706-017-0171-6.
Janssen HA. Versuche über getreidedruck in silozellen, vol. 39. Verein Deutscher Ingenieure; 1895. p. 1045–9 (in German).
Li L, Aubertin M. An improved analytical solution to estimate the stress state in sub-vertical backfilled stopes. Canadian Geotechnical Journal 2008;45(10):1487–96.
Li L, Aubertin M. Influence of water pressure on the stress state in stopes with cohesionless backfill. Geotechnical and Geological Engineering 2009a;27(1):1–11.
Li L, Aubertin M. A three-dimensional analysis of the total and effective stresses in submerged backfilled stopes. Geotechnical and Geological Engineering 2009b;27(4):559–69.
Li L, Aubertin M. Numerical investigation of the stress state in inclined backfilled stopes. International Journal of Geomechanics 2009c;9(2):52–62.
Li L, Aubertin M. An elasto-plastic evaluation of the stress state around cylindrical openings based on a closed multiaxial yield surface. International Journal for Numerical and Analytical Methods in Geomechanics 2009d;33(2):193–213.
Li L, Aubertin M. An analytical solution for the nonlinear distribution of effective and total stresses in vertical backfilled stopes. Geomechanics and Geoengineering 2010;5(4):237–45.
Li L, Aubertin M, Simon R, Bussière B, Belem T. Modeling arching effects in narrow backfilled stopes with FLAC. In: Proceedings of the 3rd international symposium on FLAC & FLAC 3D numerical modelling in geomechanics. Rotterdam: A.A. Balkema; 2003. p. 211–9.
Li L, Aubertin M, Simon R, Bussière B. Formulation and application of a general inelastic locus for geomaterials with variable porosity. Canadian Geotechnical Journal 2005;42(2):601–23.
Li L, Aubertin M, Shirazi A. Implementation and application of a new elasto-plastic model based on a multiaxial criterion to assess the stress state near underground openings. International Journal of Geomechanics 2010;10(1):13–21.
Li L, Aubertin JD, Dubé JS. Stress distribution in a cohesionless backfill poured in a silo. The Open Civil Engineering Journal 2014;8:1–8.
Marston A. The theory of external loads on closed conduits in the light of the latest experiments. Bulletin No. 96. Ames, USA: Iowa Engineering Experiment Station; 1930.
Mitchell RJ. Sill mat evaluation using centrifuge models. Mining Science and Technology 1991;13(3):301–13.
Pariseau WG, Hill JRM, McDonald MM, McNay LM. A support-performance prediction method for hydraulic backfill (No. 8161–8163). US Department of the Interior, Bureau of Mines; 1976.
Pirapakaran K, Sivakugan N. Arching within hydraulic fill stopes. Geotechnical and Geological Engineering 2007a;25(1):25–35.
Pirapakaran K, Sivakugan N. A laboratory model to study arching within a hydraulic fill stope. ASTM Geotechnical Testing Journal 2007b;30(6):496–503.
Shahsavari M, Grabinsky M. Cemented paste backfill consolidation with deposition-dependent boundary conditions. In: GeoRegina 2014. Canadian Geotechnical Society; 2014.

Shahsavari M, Moghaddam R, Grabinsky M. Liquefaction screening assessment for as-placed cemented paste backfill. In: GeoRegina 2014. Canadian Geotechnical Society; 2014.
Sobhi MA. Analyse numérique du coefficient de pression latérale des terres et des contraintes dans les chantiers miniers. MS Thesis. Montréal, Canada: École Polytechnique de Montréal; 2014.
Sobhi MA, Li L, Aubertin M. Numerical investigation of earth pressure coefficient along central line of backfilled stopes. Canadian Geotechnical Journal 2017;54(1):138–45.
Take W, Valsangkar A. Earth pressures on unyielding retaining walls of narrow backfill width. Canadian Geotechnical Journal 2001;38(6):1220–30.
Terzaghi K. Theoretical soil mechanics. New York: John Wiley & Sons, Inc.; 1943.
Thompson B, Bawden W, Grabinsky M. In situ measurements of cemented paste backfill at the Cayeli Mine. Canadian Geotechnical Journal 2012;49(7):755–72.
Ting CH, Shukla SK, Sivakugan N. Arching in soils applied to inclined mine stopes. International Journal of Geomechanics 2011;11(1):29–35.
Ting CH, Sivakugan N, Shukla SK. Laboratory simulation of the stresses within inclined stopes. Geotechnical Testing Journal 2012;35(2):280–94.
Ting CH, Sivakugan N, Read W, Shukla SK. Analytical expression for vertical stress within an inclined mine stope with non-parallel walls. Geotechnical and Geological Engineering 2014;32(2):577–86.
Veenstra RL, Grabinsky MW, Bawden WF, Thompson BD. The use of numerical modelling to determine the stress within early age cemented paste used to backfill an underground stope. In: Potvin Y, Grice AG, editors. Minefill 2014. Australian Centre for Geomechanics; 2014a. p. 97–111.
Veenstra RL, Grabinsky MW, Bawden WF, Thompson BD. A numerical analysis of how permeability affects the development of pore water pressure in early age cemented paste backfill in a backfilled stope. In: Potvin Y, Grice AG, editors. Minefill 2014. Australian Centre for Geomechanics; 2014b. p. 83–95.
Widisinghe S, Sivakugan N, Wang VZ. Laboratory investigations of arching in backfilled mine stopes. In: Leung CF, Goh SH, Shen RF, editors. Advances in geotechnical infrastructure. Singapore: Research Publishing; 2013. p. 741–6.
Widisinghe SD, Sivakugan N, Wang VZ. Loads on barricades in hydraulically backfilled underground mine stopes. In: Potvin Y, Grice AG, editors. Minefill 2014. Australian Centre for Geomechanics; 2014. p. 123–33.

Mohamed Amine Sobhi obtained MEng from École des Mines de Douai, France and MSc from École Polytechnique de Montréal, Canada in 2014. He is holder of Alexander Graham Bell Canada Graduate Scholarship provided by NSERC to pursue a doctorate at École Polytechnique de Montréal on rockbursts in underground mines.

Li Li obtained BSc from North China University of Science and Technology in 1986, MSc from Changsha Institute of Mining Research, China in 1990, and PhD from Université Paris 7 – Denis Diderot, France in 1997. From 1997 to 2008, Dr. Li worked at Polytechnique Montréal as postdoctoral researcher and Research associate. He was an expert and consulting engineer in Genivar (now WSP) between 2008 and 2010. From 2010 to 2012, Dr. Li was an associate professor at École de technologie supérieure, Montréal, Québec, Canada. Since 2012, he is Associate Professor of Department of Civil, Geological and Mining Engineering, École Polytechnique de Montréal, Montréal, Quebec, Canada. He is the author or co-author of 95 journal and conference papers. He is the reviewer of more than 15 refereed journals. Over the years, Dr. Li is particularly active in numerical modeling and analytical solution development for the design of backfilled stopes.